



THE UNIVERSITY *of* EDINBURGH

Edinburgh Research Explorer

## A Carbon Flower Based Flexible Pressure Sensor Made from LargeArea Coating

**Citation for published version:**

O'Neill, S, Gong, H, Matsuhisa, N, Chen, S, Moon, H, Wu, H-C, Chen, X, Chen, X & Bao, Z 2020, 'A Carbon Flower Based Flexible Pressure Sensor Made from LargeArea Coating', *Advanced Materials Interfaces*, vol. 7, no. 18, 2000875. <https://doi.org/10.1002/admi.202000875>

**Digital Object Identifier (DOI):**

[10.1002/admi.202000875](https://doi.org/10.1002/admi.202000875)

**Link:**

[Link to publication record in Edinburgh Research Explorer](#)

**Document Version:**

Publisher's PDF, also known as Version of record

**Published In:**

Advanced Materials Interfaces

**General rights**

Copyright for the publications made accessible via the Edinburgh Research Explorer is retained by the author(s) and / or other copyright owners and it is a condition of accessing these publications that users recognise and abide by the legal requirements associated with these rights.

**Take down policy**

The University of Edinburgh has made every reasonable effort to ensure that Edinburgh Research Explorer content complies with UK legislation. If you believe that the public display of this file breaches copyright please contact [openaccess@ed.ac.uk](mailto:openaccess@ed.ac.uk) providing details, and we will remove access to the work immediately and investigate your claim.



# A Carbon Flower Based Flexible Pressure Sensor Made from Large-Area Coating

Stephen JK O'Neill, Huaxin Gong, Naoji Matsuhisa, Shucheng Chen, Hanul Moon, Hung-Chin Wu, Xianfeng Chen, Xiaodong Chen, and Zhenan Bao\*

Flexible pressure sensors are an essential part of robotic skin for human-machine interfaces, wearables, and implantable biomedical devices. However, the desirable characteristics of high sensitivity, conformability, and good scalability are often mutually exclusive. Here, a highly sensitive and flexible pressure sensor that can be easily fabricated by coating a carbon flower and elastomer composite is presented. The composite made from uniform-sized carbon flower particles exhibits a contact-based mechanism for pressure sensing, as opposed to typical carbon black pressure sensitive composites which utilize percolation as the sensing mechanism. The contact mechanism allows for an active layer down to 13  $\mu\text{m}$ , and a bending insensitivity down to a 5.5 mm bending radius, while maintaining a high sensitivity. Furthermore, the composite is printed over a large 1 m  $\times$  2 cm pressure sensing area, showing the preparation of this sensor can be scaled to large area.

Flexible pressure sensors allow electronic skins and wearable/implantable devices to conform with the surfaces of robotic hands or human organs for sensing the surrounding environment or continuous healthcare monitoring.<sup>[1–7]</sup> Potential applications include human-machine interfaces,<sup>[8]</sup> heart and respiration rate monitoring,<sup>[9,10]</sup> prosthetics,<sup>[11]</sup> wound monitoring,<sup>[12]</sup> and artificial robotics.<sup>[13]</sup>

To date, typical flexible pressure sensors are based on an induced change in either resistance or capacitance. This is mostly attributed to elastomer deformation when pressure is applied. Recently, the sensitivity of these sensors has been significantly improved by using pyramidal or dome-shaped elastomer microstructures.<sup>[3,7,14]</sup> This allows for a high sensitivity due to a large deformation of microstructure tips with only a small force application, causing a dramatic change in capacitance. Conductive microstructures have also been demonstrated with hierarchical carbon nanotube/graphene microstructures using polydimethylsiloxane (PDMS) molds or chemical vapor deposition (CVD) techniques, which allow for a dramatic

change in contact resistance with pressure.<sup>[15,16]</sup> Another way to improve sensitivity is using a microfoam structure, where foams are easily deformed when pressure is applied. This causes either a capacitance change,<sup>[17–19]</sup> or a resistance change due to increasing connections within a conductive-foam active layer.<sup>[20–22]</sup>

As a potential alternative, printable piezoresistive composite based pressure sensors have been developed as they can be fabricated using a one-step solution process and avoid the use of costly micro/nanofabrication techniques.<sup>[23,24]</sup> Their simplicity of design allows for a roll-to-roll fabrication process that has superb scalability and cost effectiveness, thus is highly favorable for applications involving pressure sensors over a large area, such as wearable devices or electronic skins. The common mechanism is based on percolation of conducting pathways, where the elastomer is deformed, and the number of conductive pathways increases.


One drawback of printable pressure sensors is that their flexibility has been limited, which can reduce their skin conformability and biocompatibility. This is because percolation based pressure sensors require considerable thicknesses as well as high filler concentrations ( $\approx 37$  vol%) to achieve high sensitivity.<sup>[23,24]</sup> The variation of sensor performance with thickness can also be a detriment to large-scale printing and coating, where uneven thickness can be common. Although thickness insensitive pressure sensing was demonstrated by electrospinning of 2  $\mu\text{m}$  thick composites,<sup>[2]</sup> conventional printing processes such as blade coating is favorable due to the very high throughput in the large-area printing. In addition, the sensing range was limited only to 1 kPa. Recently, we developed a type of 3D hierarchical porous carbon material with flower-like

S. JK O'Neill, H. Gong, Prof. N. Matsuhisa,<sup>[†]</sup> Dr. S. Chen, Dr. H. Moon, Dr. H.-C. Wu, Prof. Z. Bao  
Department of Chemical Engineering  
Stanford University  
Stanford, CA 94305, USA  
E-mail: zbao@stanford.edu

S. JK O'Neill, Prof. X. Chen  
School of Engineering  
Institute for Bioengineering  
The University of Edinburgh  
King's Buildings, Mayfield Road, Edinburgh EH9 3JL, UK

Prof. N. Matsuhisa, Prof. X. Chen  
Innovative Centre for Flexible Devices (iFLEX)  
School of Materials Science and Engineering  
Nanyang Technological University  
50 Nanyang Avenue, Singapore 639798, Singapore

Dr. H. Moon  
School of Electrical Engineering  
Korea Advanced Institute of Science and Technology (KAIST)  
291 Daehak-ro, Daejeon 34141, Republic of Korea

 The ORCID identification number(s) for the author(s) of this article can be found under <https://doi.org/10.1002/admi.202000875>.

<sup>[†]</sup>Present Address: Department of Electronics and Electrical Engineering, Keio University, 3-14-1 Hiyoshi, Kohoku-ku, Yokohama 223-8522, Japan

DOI: 10.1002/admi.202000875

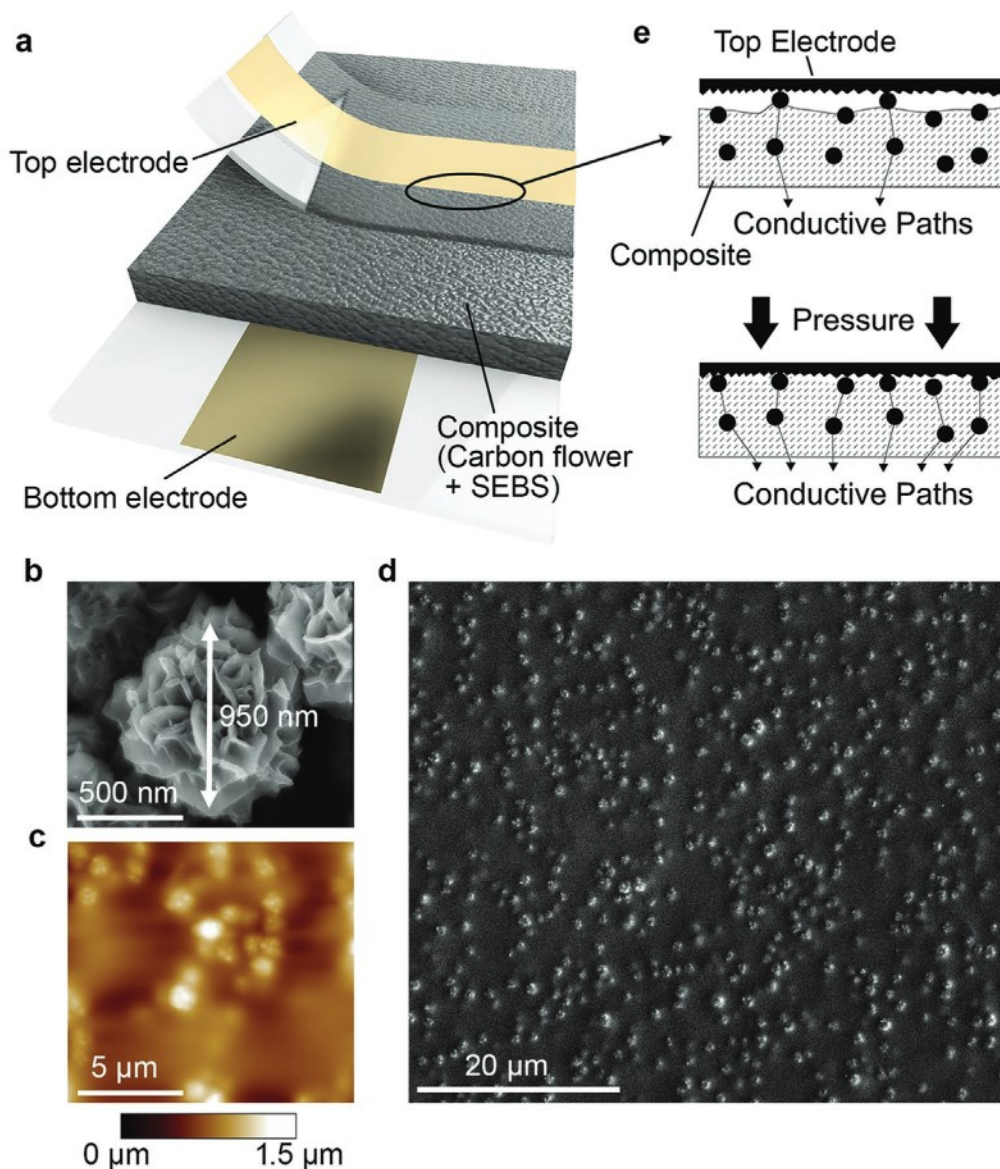


**Figure 1.** A flexible, printed pressure sensor employing a composite of carbon flower and SEBS. a) The device structure. b) An SEM image of carbon flower. c) An AFM image of the printed composite. d) An SEM image of the surface of the printed composite. e) The proposed mechanism for pressure sensing.

superstructures (carbon flowers), whose size is uniform around 950 nm average size with low dispersity.<sup>[25]</sup> We hypothesized that the carbon flowers could be used to make a printable composite with a rough surface to allow for a pressure sensor with a contact-based mechanism. By enabling a contact-based mechanism, a thin active layer can be achieved because only the interface between the electrode and composite contributes to the pressure sensing. Contact-based mechanisms also usually give fast response times, which is important for skin-mimicking applications.<sup>[26]</sup>

Here, we demonstrate a highly sensitive, flexible pressure sensor prepared by coating a composite of carbon flowers and an elastic polymer, poly(styrene-ethylene-butylene-styrene) (SEBS). The printed composite has a rough surface to enable

pressure sensors with a contact-based mechanism. The sensitivity of this type of pressure sensor is insensitive to the thickness of the composite, and similar performance is observed from a thickness of 67  $\mu\text{m}$  down to a thickness of 13  $\mu\text{m}$ . This thin active layer provides high flexibility to the pressure sensors, with a bending radius of 5.5 mm. Pressure sensors were fabricated over a large area of 1 m  $\times$  2 cm, and showed high sensitivity and dynamic range.

**Figure 1** shows the pressure sensor studied in this work. Figure 1b shows a typical scanning electron microscopy (SEM) image of our carbon flower, whose average size is around 950  $\pm$  93 nm. Conductive carbon flowers were prepared as described in the Experimental Section and our previous report.<sup>[25]</sup> As opposed to other reports of carbon flowers, our fabrication does

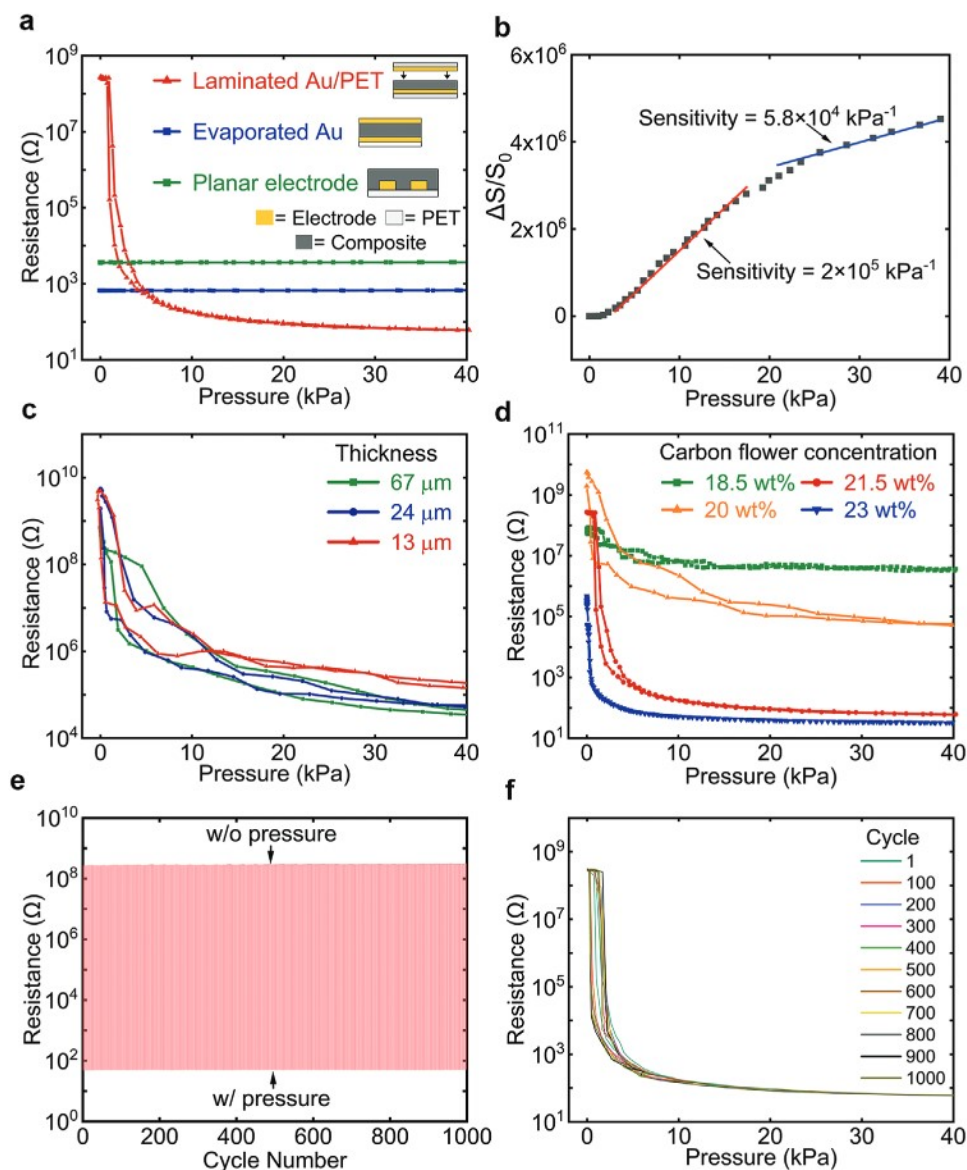


**Figure 2.** Electrical characteristics of the pressure sensor. a) Resistance–pressure characteristics to show the high sensitivity of our pressure sensor using the active layer with 21.5 wt% carbon flower. The contact-based sensing mechanism was verified by direct deposition of electrodes on the composite and by using a planar electrode configuration. b) Sensitivity characteristics of our pressure sensor in the low (0–10 kPa) and high (10–40 kPa) pressure sensing regions. c) Thickness insensitivity of the pressure sensors using active layer with 20 wt% carbon flower. d) The effect of carbon flower concentration on the pressure–resistance characteristics. e) High stability of our sensor upon cyclic pressure application. f) High reproducibility of resistance–pressure characteristics with every hundredth cycle of pressure application.

not require multistep templating and etching processes and costly reagents, which makes the materials used for our sensors compatible for low-cost, large-area fabrication.<sup>[27,28]</sup> The ink was formed by mixing carbon flowers, SEBS, and chlorobenzene, which was then printed directly onto a flexible Au/polyethylene terephthalate (PET) bottom electrode. The resulting composite film showed well-dispersed carbon flower in the SEBS matrix, which can be seen in a cross-sectional SEM image of the film in Figure S1 (Supporting Information). The surface has a rough structure as shown by an atomic force microscope (AFM) image (Figure 1c), and SEM image (Figure 1d), with a root mean square (rms) of 132 nm and an arithmetical mean

deviation (Ra) of 104 nm. The formed rough surface enables a highly sensitive contact resistance-based pressure sensor. The fabrication of the pressure sensor was completed by the lamination of a second Au/PET electrode to form the top contact, as shown in Figure 1a.

The high sensitivity of our pressure sensor is shown in Figure 2a. The composite layer consists of 21.5 wt% (15.5 vol%) carbon flower and has a thickness of 67  $\mu\text{m}$ . The resistance dramatically changes from  $2.7 \times 10^8$  to  $180 \Omega$  with a pressure of 10 kPa. The minimum force which can be sensed by this sensor is as small as 0.025 N (2.55 g in  $5 \times 5 \text{ mm}^2$ ). The sensitivity (defined as  $\partial(\Delta S/S_0)/\partial P$ , where  $\Delta S$  is the conductance

change upon applied pressure of  $P$ , and  $S_0$  is the initial conductance without applied pressure) is as high as  $2 \times 10^5 \text{ kPa}^{-1}$  in the low-pressure region (0–10 kPa), and  $5.8 \times 10^4 \text{ kPa}^{-1}$  in the high-pressure region (10–40 kPa), as shown in Figure 2b. This value is much higher than recent reports on highly sensitive pressure sensors,<sup>[6,29,30]</sup> and can be attributed to a significantly small  $S_0$  due to low initial contact (further discussion has been provided in the Supporting Information and Table S1, Supporting Information). This high sensitivity could not be obtained using other common conducting fillers. For example, pressure sensors were fabricated in a similar manner using different conducting fillers, which included spherical Ni-powder (NOVAMET Type 4SP, diameter  $\approx 10 \mu\text{m}$ ) and carbon black (TIMCAL Super C65, diameter  $\approx 70 \mu\text{m}$ ).<sup>[23,31]</sup> However, these sensors showed resistance variation of  $\approx 10^2 \Omega$  upon pressure application, which is much smaller compared to the  $\approx 10^7 \Omega$  variation of the carbon flowers based sensors (Figure S2, Supporting Information). This highlights the importance of the carbon flowers which have a unique rough structure and mono-disperse size distribution.

The sensing mechanism was confirmed to be based on the contact between composite and the top electrode by three experiments. The first experiment was to directly deposit 50 nm of Au on the composites by thermal evaporation. This gave a comparison where initially there was full contact with carbon flower. As shown in Figure 2a, the sensor made by this approach showed almost no piezoresistive response ( $0.93 \Omega$  with 40 kPa pressure application), while sensors made by lamination showed a large change of resistance ( $1.9 \times 10^8 \Omega$  with 40 kPa pressure application). Another test to determine the materials piezoresistivity was by using a planar electrode configuration. The composite was printed over planar interdigitated electrodes with a line spacing of  $10 \mu\text{m}$ . Similarly, this showed little resistance change as a function of pressure, and revealed that bulk resistance through the composite is almost consistent regardless of pressure.

The contact-based sensing mechanism was further confirmed by varying the thickness of the composite. Three different thicknesses were printed, and the thickness of each was measured using cross-sectional SEM images (Figure S1, Supporting Information). Figure 2c shows that even at the lowest thickness of  $13 \mu\text{m}$  the overall sensor performance is largely unaffected, which to our knowledge is the thinnest printed composite pressure sensor that has been demonstrated to date (as shown in Table S1, Supporting Information). The minimum thickness is currently limited by the accuracy of the blade coater. The use of blade coaters that have improved height control accuracy would enable a thinner coating. Such a thin active layer was achieved because only the interface between the electrode and composite contribute to the pressure sensing. Furthermore, the ability to make a very thin composite while maintaining high sensitivity is highly advantageous for wearable applications as the reduced thickness improves the conformability.<sup>[32]</sup> An insensitivity to thickness is also highly analogous to large-area printing fabrication, where it is difficult to achieve uniform thickness.

Figure 1e summarizes the sensing mechanism of our carbon flower-based pressure sensor. At low pressure, there is poor contact of the top electrode with the conductive carbon flower

resulting in few possible electrically conducting paths. As pressure is increased, the SEBS elastomer is deformed, which results in greater contact with the surface carbon flowers and drastically increases the number of potential conducting paths.

The sensitivity and resistance characteristics of the sensor could be tuned by varying the carbon flower concentration in the composite (Figure 2d). When the concentration is as low as 18 wt%, the sensor showed small piezoresistivity. The resistance changed from  $8.5 \times 10^7$  to  $3.4 \times 10^6 \Omega$  from a pressure application of 40 kPa. When the concentration is as high as 23 wt%, the resistance changed from  $4.7 \times 10^5 \Omega$  at 0 kPa to  $32 \Omega$  at 40 kPa. Above all, 21.5 wt% carbon flower gave the best dynamic range as the performance was described above. All subsequent tests are based on films prepared with a 21.5 wt% carbon flower loading. It is important to note that this filler concentration (21.5 wt%, 15.5 vol%) is considerably lower compared to traditional piezoresistive based composite sensors, which require high filler concentration ( $\approx 37\%$  vol%) to achieve comparable sensitivity.<sup>[23,24]</sup> The lower filler amount can potentially result in a more flexible sensor with the same thickness.

The excellent sensitivity of our pressure sensor is highly reproducible and stable over many cycles of pressure application. We conducted a stability test comprising of 1000 consecutive cycles. Figure 2e,f shows the resistance of the sensor with and without pressure as well as the pressure–resistance dynamic curve of every hundredth cycle, respectively. The on/off ratio and dynamic curve profile remain constant throughout the test, showing reliable and reproducible pressure detection.

Furthermore, our pressure sensor enabled high consistency under bending down to a 5.5 mm bending radius. This was tested by conforming the sensor to a given bending radius by bending it around a cylinder, as depicted in Figure 3a. By varying the radius of the cylinder, bending radius of 13.5, 8.35, and 5.5 mm was applied to the pressure sensor. Pressure was evenly distributed across the pressure sensing area by using a soft PDMS (prepolymer:crosslinker ratio of 50:1) which was able to conform to the top surface of the sensor. The resistance response to pressure at various bending radii is shown in Figure 3b. The high sensitivity of our sensor in the low-pressure regime caused the initial resistance to become lower ( $6.8 \times 10^3 \Omega$ ), due to the small pressure force needed to conform the sensor to the curved surface. Nonetheless, bending to different radius had minimal effect on the resistance–pressure characteristics of our sensors. The sensitivity at different bending radius

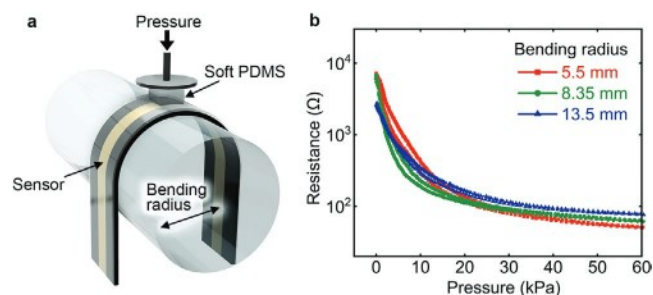


**Figure 3.** Flexibility testing of the sensor. a) A 3D schematic of the experimental setup. b) Resistance–pressure characteristics with varying bending radii.

is shown in Figure S3 (Supporting Information). The insensitivity is attributed to the contact-based mechanism, which does not suffer from the mechanical deformation that occurs at the bulk of the composite. In addition, our pressure sensor has a thin active layer that reduces the vertical force upon bending, while most printed/nonprinted pressure sensors require a thick active layer.<sup>[2]</sup> Pressure sensing while bending is important, as it is the most common case for actual application in wearables or robotics.

The demonstrated flexibility of our pressure sensors is high compared with previous reports of printable pressure sensors. Most of the previous reports showed the ability of sensors to flex but the sensing tests were performed in a flat state.<sup>[24,33,34]</sup> It is important to discuss that bending insensitivity was shown using 2  $\mu\text{m}$  thick nanofiber composites prepared by electrospinning, which is different from conventional high-throughput printing processes.<sup>[2]</sup> Moreover, the testing method did not precisely apply pressure to samples with different bending radius. It applied a point force by using two metal bars intersected, which means the same pressure is applied to the same area even if the bending radius is changed. In addition, the pressure sensing range was limited to only 1 kPa, while most reported sensors can sense pressure larger than 10 kPa (Table S1, Supporting Information).

In addition to the desirable characteristics of performance being insensitive to thickness, our pressure sensors are printable and highly compatible with large-scale manufacturing. To demonstrate this, we printed the composite ink over a 1 m long and 2 cm wide ITO/PET tape substrate. A picture of the sample has been given in Figure 4a. The sensor is fabricated by simply

placing a second ITO/PET film directly on top of the composite, which is simple and scalable to large area. The performance of the pressure sensor was tested at 15 cm increments along the printed layer. Each of the five samples gave consistent pressure sensing dynamic range, as shown in Figure 4b. A linear plot of the samples has also been given in Figure S4 (Supporting Information) to clearly show the variance. The relative standard deviation of the samples' resistance is only 13% at 10 kPa. Although the relative standard deviation at 0 kPa is as high as 74%, this is caused by the very high sensitivity of our sensors at low pressure regime, which can be easily fixed by the improvement of top electrodes lamination. Compared to previous testing with Au/PET electrodes, the high sheet resistance of ITO limited the dynamic range. The use of more conductive metal electrodes could easily solve this issue. This fabrication process for the proposed composite based pressure sensor is compatible to roll-to-roll based manufacturing, thus is readily useful to make highly sensitive pressure sensors for very low cost, which can realize distributed pressure sensor networks for the Internet of Things (IoT).

We have demonstrated a highly sensitive pressure sensor, which shows high flexibility and can be printed over a large area. This is attributed to the contact-based mechanism, which allows for a thin film active layer and does not suffer from the mechanical deformation that occurs to the bulk of the composite. Our flexible, large-area, and highly sensitive pressure sensors should inspire applications in the field of large-area electronic skins to conformably cover large-area skins of humans or robots as well as IoT applications.

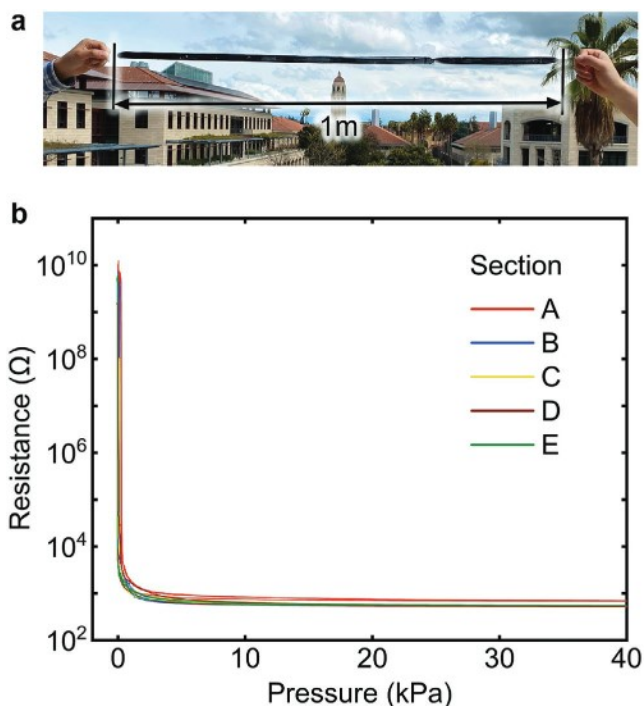


**Figure 4.** Large-area printing of sensor. a) A photo of the large area 1 m  $\times$  2 cm printing sample. b) Resistance–pressure characteristics of sensors taken at 15 cm increments along the sample.

## Experimental Section

**Synthesis of Carbon Flower Particles:** Conductive carbon flowers were prepared as outlined by a previous report.<sup>[25]</sup> Polyacrylonitrile flowers were first prepared via a free radical polymerization using acrylonitrile as the monomer, azobis(isobutyronitrile) (AIBN) as the initiator, and acetone as the solvent. Acrylonitrile (5 mL), acetone (5 mL), and AIBN (5 mg) were added to a vial. The vial was heated up to 70  $^{\circ}\text{C}$  and held for 12 h under nitrogen protection without stirring. The resultant white powder consisted of polyacrylonitrile flower particles and was dried in vacuum oven at 50  $^{\circ}\text{C}$  for overnight. To convert polyacrylonitrile flowers to carbon flowers, they were firstly stabilized in air at 230  $^{\circ}\text{C}$  for 2 h with a ramping rate of 0.1  $^{\circ}\text{C min}^{-1}$ . The stabilized flowers were then carbonized in nitrogen (70 sccm) at 1000  $^{\circ}\text{C}$  for 2 h with a ramping rate of 2  $^{\circ}\text{C min}^{-1}$ . This method produced carbon flowers with an average size of 950 nm.

**Fabrication of Carbon Flower Pressure Sensor:** In order to ensure uniform dispersion of carbon flowers in the SEBS embedding elastomer, the carbon flowers were first ground with a mortar and pestle. Carbon flowers (55 mg) were then dispersed in chlorobenzene solvent (1 mL) by sonicating overnight, followed by adding SEBS (200 mg, Asahi-Kasei, H1052) and speed mixing at 3000 rpm for 5 min. To ensure that the SEBS was fully dissolved, the solution was placed in an oven at 70  $^{\circ}\text{C}$  overnight. Following a second speed mix at 3000 rpm for 5 min, the composite mixture could then be printed directly onto a flexible Au/PET bottom electrode. The Au/PET electrodes were fabricated by evaporating 50-nm-thick Au onto PET with 5-nm-thick Cr adhesion layer. Printing was done using a fixed height blade which deposited a coating onto the electrode. The composite was then left to dry overnight. The resulting composite film showed well-dispersed carbon flower in the SEBS matrix, which can be seen in a cross-sectional SEM of the film in Figure S1 (Supporting Information). Once dry, a second identical Au/PET electrode

could be laminated to form the top contact, as shown in Figure 1c. For large-area printing, the active layer was deposited using a fixed blade height onto a 1 m long ITO/PET substrate. The characterization of large-area sensors was also conducted by laminating another ITO/PET film.

*Electrical Characterization of Pressure Sensors:* Agilent E4980A Precision LCR meter was used to measure the resistance between the top and bottom electrodes at 1 kHz frequency and with a 1 V AC signal. Meanwhile, the pressure was measured using a force gauge (Dillion GL model, 0.5 g resolution) and pressure was applied by using a motorized z-axis stage. A step size of 2  $\mu\text{m}$  to a maximum force of 2 N was applied to all of the sensors. To ensure that pressure was evenly distributed to the sensor area, a  $0.5 \times 0.5 \text{ cm}^2$  of PDMS was placed between the pressure sensor and the force gauge. SEM images were collected using FEI Magellan 400 XHR SEM with 5 kV acceleration voltage. AFM images were collected using Nanoscope III Digital Instruments/Veeco Metrology Group.

## Supporting Information

Supporting Information is available from the Wiley Online Library or from the author.

## Acknowledgements

S.J.K.O'N., H.G., N.M., and S.C. contributed equally to this work. N.M. was supported by the Japan Society for the Promotion of Science (JSPS) overseas research fellowship. This work was supported by the Beijing Institute of Collaborative Innovation (BICI). Part of this work was performed at the Stanford Nano Shared Facilities (SNSF), supported by the National Science Foundation under Award No. ECCS-1542152.

## Conflict of Interest

The authors declare no conflict of interest.

## Keywords

composite, flexible electronics, pressure sensors, printed electronics

Received: May 18, 2020

Revised: June 18, 2020

Published online: July 30, 2020

- [1] C. Wang, D. Hwang, Z. Yu, K. Takei, J. Park, T. Chen, B. Ma, A. Javey, *Nat. Mater.* **2013**, *12*, 899.
- [2] S. Lee, A. Reuveny, J. Reeder, S. Lee, H. Jin, Q. Liu, T. Yokota, T. Sekitani, T. Isoyama, Y. Abe, Z. Suo, T. Someya, *Nat. Nanotechnol.* **2016**, *11*, 472.
- [3] S. C. B. Mannsfeld, B. C. K. Tee, R. M. Stoltenberg, C. V. H. H. Chen, S. Barman, B. V. O. Muir, A. N. Sokolov, C. Reese, Z. Bao, *Nat. Mater.* **2010**, *9*, 859.
- [4] N. Luo, Y. Huang, J. Liu, S. C. Chen, C. P. Wong, N. Zhao, *Adv. Mater.* **2017**, *29*.
- [5] D. J. Lipomi, M. Vosgueritchian, B. C. K. Tee, S. L. Hellstrom, J. A. Lee, C. H. Fox, Z. Bao, *Nat. Nanotechnol.* **2011**, *6*, 788.
- [6] L. Pan, A. Chortos, G. Yu, Y. Wang, S. Isaacson, R. Allen, Y. Shi, R. Dauskardt, Z. Bao, *Nat. Commun.* **2014**, *5*, 3002.
- [7] B. C.-K. Tee, A. Chortos, R. R. Dunn, G. Schwartz, E. Eason, Z. Bao, *Adv. Funct. Mater.* **2014**, *24*, 5427.
- [8] M. Kang, J. Kim, B. Jang, Y. Chae, J. H. Kim, J. H. Ahn, *ACS Nano* **2017**, *11*, 7950.
- [9] Y. Huang, Y. Chen, X. Fan, N. Luo, S. Zhou, S.-C. Chen, N. Zhao, C. P. Wong, *Small* **2018**, *14*, 1801520.
- [10] K. Y. Shin, J. S. Lee, J. Jang, *Nano Energy* **2016**, *22*, 95.
- [11] A. P. Gerratt, H. O. Michaud, S. P. Lacour, *Adv. Funct. Mater.* **2015**, *25*, 2287.
- [12] W. J. Deng, L. F. Wang, L. Dong, Q. A. Huang, *IEEE Sens. J.* **2018**, *18*, 4886.
- [13] C. Bartolozzi, L. Natale, F. Nori, G. Metta, *Nat. Mater.* **2016**, *15*, 921.
- [14] B. Zhu, Z. Niu, H. Wang, W. R. Leow, H. Wang, Y. Li, L. Zheng, J. Wei, F. Huo, X. Chen, *Small* **2014**, *10*, 3625.
- [15] M. Jian, K. Xia, Q. Wang, Z. Yin, H. Wang, C. Wang, H. Xie, M. Zhang, Y. Zhang, *Adv. Funct. Mater.* **2017**, *27*, 1606066.
- [16] K. Xia, C. Wang, M. Jian, Q. Wang, Y. Zhang, *Nano Res.* **2018**, *11*, 1124.
- [17] S. Wan, H. Bi, Y. Zhou, X. Xie, S. Su, K. Yin, L. Sun, *Carbon* **2017**, *114*, 209.
- [18] M. Pruvost, W. J. Smit, C. Monteux, P. Poulin, A. Colin, *NPJ Flexible Electron.* **2019**, *3*, 7.
- [19] D. Kwon, T. I. Lee, J. Shim, S. Ryu, M. S. Kim, S. Kim, T. S. Kim, I. Park, *ACS Appl. Mater. Interfaces* **2016**, *8*, 16922.
- [20] A. Tewari, S. Gandla, S. Bohm, C. R. McNeill, D. Gupta, *ACS Appl. Mater. Interfaces* **2018**, *10*, 5185.
- [21] W. Liu, N. Liu, Y. Yue, J. Rao, C. Luo, H. Zhang, C. Yang, J. Su, Z. Liu, Y. Gao, *J. Mater. Chem. C* **2018**, *6*, 1451.
- [22] W. Huang, K. Dai, Y. Zhai, H. Liu, P. Zhan, J. Gao, G. Zheng, C. Liu, C. Shen, *ACS Appl. Mater. Interfaces* **2017**, *9*, 42266.
- [23] G. Canavese, M. Lombardi, S. Stassi, C. F. Pirri, *Appl. Mech. Mater.* **2012**, *110*, 1336.
- [24] D. Lee, H. Lee, Y. Jeong, Y. Ahn, G. Nam, Y. Lee, *Adv. Mater.* **2016**, *28*, 9364.
- [25] S. Chen, D. M. Koshy, Y. Tsao, R. Pfattner, X. Yan, D. Feng, Z. Bao, *J. Am. Chem. Soc.* **2018**, *140*, 10297.
- [26] S. Li, Y. Zhang, Y. Wang, K. Xia, Z. Yin, H. Wang, M. Zhang, X. Liang, H. Lu, M. Zhu, H. Wang, X. Shen, Y. Zhang, *InfoMat* **2020**, *2*, 184.
- [27] L. Zhou, T. Huang, A. Yu, *ACS Sustainable Chem. Eng.* **2014**, *2*, 2442.
- [28] Z. Xu, X. Zhuang, C. Yang, J. Cao, Z. Yao, Y. Tang, J. Jiang, D. Wu, X. Feng, *Adv. Mater.* **2016**, *28*, 1981.
- [29] Z. Wang, S. Wang, J. Zeng, X. Ren, A. J. Y. Chee, B. Y. S. Yiu, W. C. Chung, Y. Yang, A. C. H. Yu, R. C. Roberts, A. C. O. Tsang, K. W. Chow, P. K. L. Chan, *Small* **2016**, *12*, 3827.
- [30] N. Bai, L. Wang, Q. Wang, J. Deng, Y. Wang, P. Lu, J. Huang, G. Li, Y. Zhang, J. Yang, K. Xie, X. Zhao, C. F. Guo, *Nat. Commun.* **2020**, *11*, 1.
- [31] L. Wang, T. Ding, P. Wang, *IEEE Sens. J.* **2009**, *9*, 1130.
- [32] D.-H. Kim, J. Viventi, J. J. Amsden, J. Xiao, L. Vigeland, Y.-S. Kim, J. A. Blanco, B. Panilaitis, E. S. Frechette, D. Contreras, D. L. Kaplan, F. G. Omenetto, Y. Huang, K.-C. Hwang, M. R. Zakin, B. Litt, J. A. Rogers, *Nat. Mater.* **2010**, *9*, 511.
- [33] J. Wang, J. Jiu, M. Nogi, T. Sugahara, S. Nagao, H. Koga, P. He, K. Suganuma, *Nanoscale* **2015**, *7*, 2926.
- [34] H. Kim, G. Kim, T. Kim, S. Lee, D. Kang, M. S. Hwang, Y. Chae, S. Kang, H. Lee, H. G. Park, W. Shim, *Small* **2018**, *14*, 1.